Front. Optoelectron. 2016, 9(3): 346–352
DOI 10.1007/s12200-016-0597-0

RESEARCH ARTICLE

Principle and applications of semiconductor optical amplifiers-based turbo-switches

Xuelin YANG (✉), Weisheng HU

State Key Laboratory of Advanced Optical Communication Systems and Networks, Shanghai Jiao Tong University, Shanghai 200240, China

Abstract All-optical high-speed turbo-switches can effectively increase the switching speed using cascaded semiconductor optical amplifiers (SOAs). The overall recovery time or the bandwidth of turbo-switch was numerically analyzed with time-domain and frequency-domain SOA models. The turbo-switch was explored from the fundamental carrier dynamics in SOAs for the purpose of further increasing its operation speed. An integrated turbo-switch was also been proposed and demonstrated, where a phase adjustable Mach-Zehnder interferometer (MZI) was applied as an optical band-pass filter between SOAs. Wavelength conversion was first demonstrated at 84.8 Gbit/s using the integrated turbo-switch.

Keywords semiconductor optical amplifier (SOA), all-optical signal processing, high-speed switches, semiconductor integration

1 Introduction

Currently, optical communication networks rely mainly on electronic digital signal processing, which leads to the loss of transparency, high power consumption & cost, and the complexity due to the repeated optical-electric-optical (O-E-O) conversion. All-optical signal processing functions such as wavelength conversion, regeneration and logic gates, may be implemented using semiconductor optical amplifiers (SOAs), are potentially practical alternatives in the future high-speed optical fiber networks. SOA is regarded as one of the key nonlinear optical devices for all-optical high-speed logic and switches, however the inherent SOA recovery time (~100 ps) limits its application for ultrafast optical data signals. A number of schemes have been proposed to enhance the operation speed of SOA-based all-optical devices, for instance, differential cross-phase modulation (XPM) using SOA interferometer [1], or a biased narrow band-pass filter to spectrally select one of the side-bands (blue-shifted or red-shifted) of the output signal [2]. The wavelength conversion at 320 Gb/s was reported via the chirp effect on the SOA output associated with the SOA ultrafast gain dynamics [2]. However, the optical signal-to-noise ratio (OSNR) of the output signal was degraded to a large extent since the optical carrier was suppressed. To increase the overall operation speed while keeping the OSNR higher, turbo-switch was proposed first in 2006 [3], which incorporated two cascaded SOAs and one wide optical band-pass filter (OBF) between SOAs. It has been demonstrated that error-free wavelength conversion at 170 Gbit/s was achieved using discrete two SOAs.

In this paper, the progress on SOA-based turbo-switch was reviewed in details by SOA models established within both of the time- and frequency-domains, in order to understand its operation principle, optimal parameters and the ultimate operation speed. Furthermore, a novel integrated version of turbo-switch was proposed and fabricated, where a Mach-Zehnder interferometer (MZI) can be functioned as OBF to block the data (pump) signal, while the phase difference between the MZI arms can be adjusted by the applied current to the two saturated SOAs in two MZI arms. It was demonstrated for the first time that, wavelength conversion at 84.8 Gbit/s was successfully achieved using the integrated turbo-switch.

2 Time-domain modeling of turbo-switch

The schematic experimental setup of turbo-switch is shown in Fig. 1, which is consisted of two cascaded SOAs with a broad band-pass filter (~3 nm in experiments) between them [4].The pump pulse and continuous wave (CW) probe are combined as the input to the first SOA (SOA1). The function of the filter is simply to filter out the pump pulses and allow only the modulated CW beam to pass through the second SOA (SOA2).

Received January 8, 2016; accepted April 2, 2016

E-mail: x.yang@sjtu.edu.cn

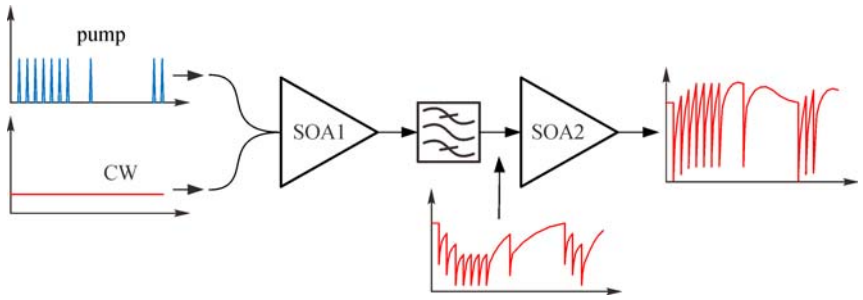

Fig. 1 Schematic setup of turbo-switch

The SOA rate equations for the total carrier density dynamics are all taken into consideration, which related to the (inter-band) band-filling effect and the local carrier density variations, which are associated by the ultrafast (intra-band) effects, such as the carrier heating (CH) and spectrum hole burning (SHB) process. Traveling-wave rate equations in terms of the optical power and phase, derived from Maxwell equations and Kramers-Kronig relations, are also incorporated in the SOA model to obtain the amplitude/phase of the optical pulses propagating through SOA, which can be expressed as follows [4,5]

$$\frac{\partial N(z,t)}{\partial t} = \frac{I}{eV} - R(N(z,t)) - v_g g S(z,t) - v_g g_{ase}[S^+_{ase}(z,t) + S^-_{ase}(z,t)], \quad (1)$$

$$\frac{\partial n_{CH}(z,t)}{\partial t} = -\frac{n_{CH}(z,t)}{\tau_{CH}} - \frac{v_g \varepsilon_{CH}}{a_0 \tau_{CH}} g S(z,t), \quad (2)$$

$$\frac{\partial n_{SHB}(z,t)}{\partial t} = -\frac{n_{SHB}(z,t)}{\tau_{SHB}} - \frac{v_g \varepsilon_{SHB}}{a_0 \tau_{SHB}} g S(z,t) - \left[\frac{\partial N(z,t)}{\partial t} + \frac{\partial n_{CH}(z,t)}{\partial t}\right], \quad (3)$$

where the first term in the right hand side of Eq. (1) represents the increase of the total carrier density due to the injected current I to the SOA. Here, we have assumed a uniform distribution of the injected current along the longitude. In Eqs. (1)–(3), various parameters are taken from Ref. [4,5], while e is the electron charge, V is the volume of the active region in the SOA, v_g is the group velocity. g is the gain coefficient, S is the photon density in the active region, g_{ase} is the equivalent gain coefficient for the amplified spontaneous emission (ASE), τ_{CH} and ε_{CH} in Eq. (2) are carrier-carrier relaxation time and gain suppression factor caused by CH, while τ_{SHB} and ε_{SHB} in Eq. (3) are temperature relaxation time and gain suppression factor caused by SHB.

The gain dynamics of a single SOA and turbo-switch are plotted in Fig. 2. An obvious reduction of the gain recovery time is obvious in the gain curve of turbo-switch compared

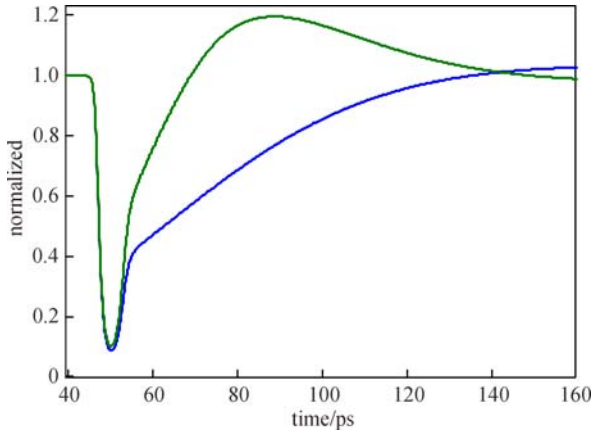

Fig. 2 Normalized gain dynamics of a single SOA (blue) and turbo-switch (green)

with the case of a single SOA, which decreases from ~100 to 20 ps, ~4 times shorter than a single SOA. The simulation result is consistent with the experimental results presented in Ref. [3]. As a consequence, the slow recovering tail of SOA1 is getting compensated by SOA2, thus the overall recovery time of turbo-switch becomes significantly shorter.

If more SOAs are cascaded similar to turbo-switch, is there any further improvement to the operation speed? The simulation results of the gain recovery time and normalized overshoot level as a function of SOA stage are given and plotted in Fig. 3. The results are actually encouraging, since the recovery time can be further reduced to ~10 ps when three SOAs are cascaded. It implies that more SOAs are cascaded, faster recovery could be expected. However, the level of the gain overshoot (right-hand axis) also rise almost linearly as the numbers of SOA increases, whereas the recovery time is not reduced significantly any more when the number of SOAs > 5.

3 Frequency-domain modeling of turbo-switch

The frequency-domain SOA model is adopted based on the

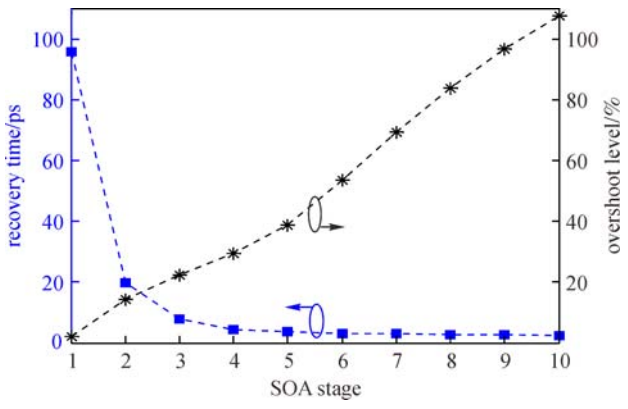

Fig. 3 Recovery time and overshoot level as a function of the number of the cascading SOAs

theory of small-signal analysis presented in Refs. [6,7]. The time-domain parameters such as optical power, optical phase shift and SOA carrier density can be generally expressed in terms of the steady term of $X(t)$ and the perturbation term $\Delta X(t)$. The power, phase evolution of the optical data signal ($i = 1$) and the CW ($i = 2$) are

$$\frac{\partial \Delta P_i}{\partial z} = (g-\alpha_{\text{int}})\Delta P_i + \frac{-\frac{g\overline{P}_i}{P_{\text{sat}}}\sum_i \Delta P_i}{1/\tau_{\text{eff}} + \text{j}\omega}, \quad (4)$$

$$\frac{\partial \overline{P}_i}{\partial z} = (g-\alpha_{\text{int}})\overline{P}_i, \quad (5)$$

$$\frac{\partial \Delta \phi_i}{\partial z} = -\frac{1}{2}\alpha_H \frac{(-g)}{P_{\text{sat}}(1/\tau_{\text{eff}} + \text{j}\omega)} \sum_i \Delta P_i, \quad (6)$$

where α_H is the linewidth enhancement factor, g and α_{int} are the gain and internal waveguide loss coefficients of SOA respectively, and τ_{eff} is the effective lifetime. Other parameters are defined as the same in Ref. [6]. The ratio of the CW perturbation over the control data perturbation ΔP_1 is defined as small-signal frequency response (SSFR, $\eta(\omega)$), which shows the frequency transfer function of the optical device. From Eqs. (4)–(6), SSFR of turbo-switch can be obtained.

We have simulated the SSFRs at various positions in the setups plotted in Fig. 4, where different placements of SOAs along with a delay-interferometer (DI, with a differential delay of 3 ps) are compared. Figure 5(a) shows the normalized SSFRs of a single SOA, turbo-switch and turbo-switch followed by a DI, which are plotted as the positions "A", "B" and "E" in Fig. 4. It can be noted that, the 3dB bandwidth of turbo-switch increases ~4 times if compared with a single SOA. In the case of a DI placed between (position "D" in Fig. 4) and after (position "E" in Fig. 4) two SOAs, the corresponding normalized SSFRs are presented in Fig. 5(b). Comparing the curves in Fig. 5(b), it is beneficial to place the DI between two SOAs, owing to much lower overshoots for curve "D" in the range of 3-dB frequency bandwidth. This is in good agreement with the experimental results, where the output pulse quality of the case "D" was better [8]. In Fig. 5(b), the 3 dB bandwidth of the SSFR can reach up to ~300 GHz, which implies that the potential operation speed of turbo-switch can be > 300 Gbit/s. In addition, two overshoots around 4 and 300 GHz are obviously presented in the SSFR curves in the case of the combination of turbo-switch and DI.

4 Integrated turbo-switch design

The proposed integrated turbo-switch consists of two cascading SOAs and a filter between two SOAs to block the data pump signal [3], as shown in Fig. 6. The difficulty lies in how to design an integrated OBF to block the data wavelength while allow the CW probe signal to pass through. The SOA-MZI was proposed and applied as the OBF, which can be tuned to pass the CW signal and filter out the data signal via adjusting the currents of SOAs in the MZI arms. Since the SOAs were operated in saturation regime, the SOA gain was constant, so the current variation

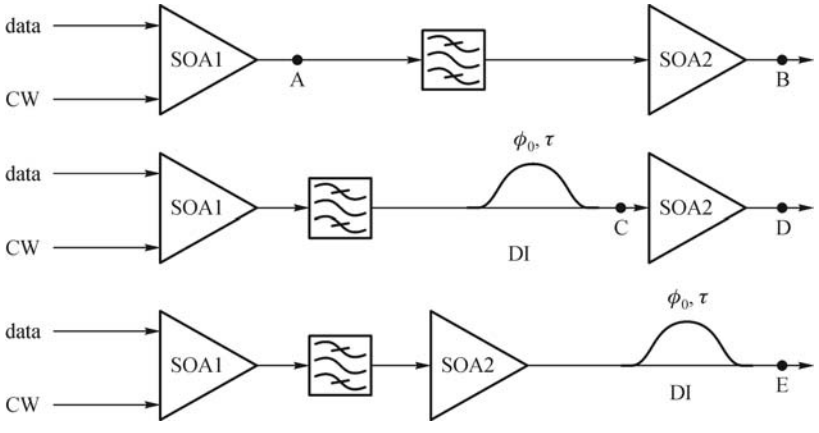

Fig. 4 Structure of turbo-switch only (top), with a DI before SOA2 (middle) and with a DI after SOA2 (bottom)

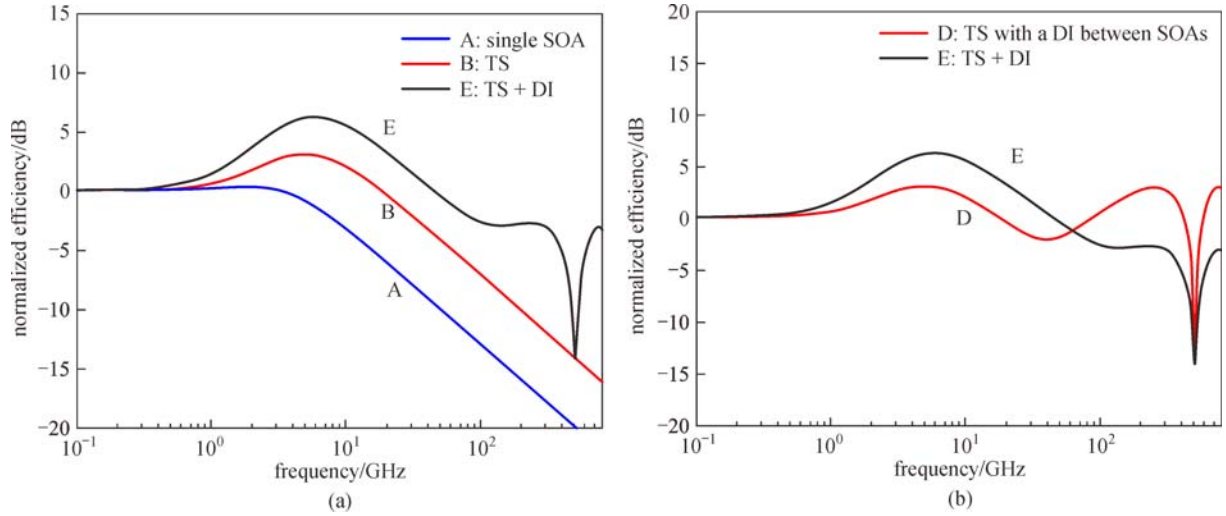

Fig. 5 Normalized SSFR of a single SOA, turbo-switch and a turbo-switch, (a) followed by a DI; (b) with a DI between two SOAs, corresponding to the setups shown in Fig. 4

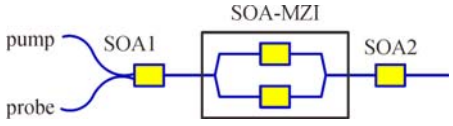

Fig. 6 Structure of the proposed integrated turbo-switch

did not change the amplitude of the output optical signal traveled through the MZI arms.

We have designed and fabricated a few turbo-switch chips, and performed some primary measurements to verify the device functionalities.

4.1 Performance of optical band-pass filter

The OBF was designed to be tunable with respect to the input optical wavelength. The optical phase can be adjustable by changing the bias currents of SOAs inside MZI arms. The measured phase difference between two arms of the MZI is plotted in Fig. 7, where the bias current of upper MZI arm was kept unchanged, and the bias current of lower arm was then changed from 400 to 850 mA with an increment of 15 mA at each step. As indicated in Fig. 7, the phase difference between two MZI arms for the optical signal at 1550 nm was easy to obtain π radians via changing the bias current. However the SOA gain was kept in saturation, so the optical power after MZI did not change. Furthermore, since the phase difference was different with respect to the input optical wavelength. It was also verified by the measurement of the optical spectra of the pump and probe signals, as shown in Fig. 8, where the pump at 1550 nm was suppressed ~25 dB, while the CW was reduced ~15 dB. As a result, the peak of CW probe signal was more than 10 dB higher than the pump signal after MZI, which implies the MZI was suitable to be employed as OBF in turbo-switch.

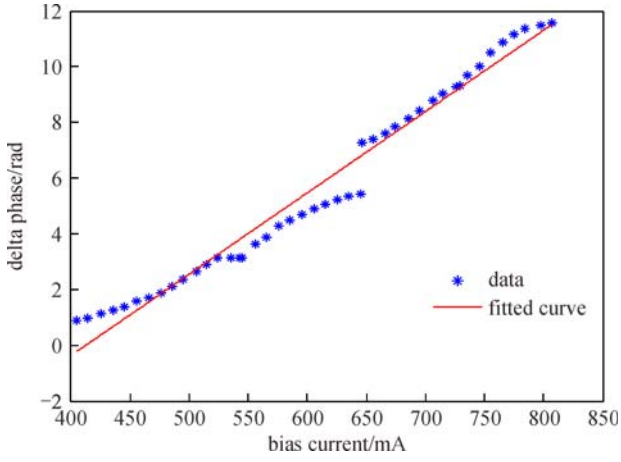

Fig. 7 Phase difference between two MZI arms versus bias SOA current

4.2 Dynamics of integrated turbo-switch

The measured gain dynamics of the integrated turbo-switch is shown in Fig. 9, where the gain curves were obtained versus the various applied currents to SOAs (SOA1 and SOA2). In Fig. 9, the turbo-switch reduced its gain recovery time when the bias current to the SOAs was higher, which indicated that, the SOA2 usually has to be kept in saturation state for SOAs [8–10]. When the bias current was high enough, an overshoot in the gain curve was evident, which implied the effective compensation of the patterning effect by SOA2. In contrast, when the bias currents to SOAs were low (~100 mA), SOA2 was unsaturated, the overall gain recovery time was not reduced significantly, which was similar to the case of a single SOA. It should be noted that, the bias current can be used as the adjustment for the level of overshoot, which could be applied to compensate the tail of SOA gain

recovery; therefore, the overall gain of the turbo-switch should be optimized by adjusting the bias currents of the two SOAs.

As a straight-forward result of the overall shorter recovery time of turbo-switch, the pattern effect can be mitigated [4]. To verify the pattern effect of integrated turbo-switch, the output patterns of a CW probe modulated by a pump pulse train of 2 ps (full width at half maximum, FWHM) at 42.4 Gbit/s for different bias currents, is shown in Fig. 10. It can be observed that, the top and bottom patterns in Fig. 10 experiences a constantly lower or higher in trend, while the middle has a relatively flat bottom in the case of inputting a consequent "1". The three patterns in Fig. 10 corresponded to the three status of SOA2: unsaturated, saturated and over-saturated respectively, which was in good agreement with the reported experimental results obtained from discrete turbo-switches [3] as well as the simulation results [4,8].

5 Wavelength conversion using integrated turbo-switch

The experimental setup is shown in Fig. 11, where the pump data was a 2^7–1 pseudo-random binary sequence (PRBS), and the pump pulse train was made by 2 ps (FWHM) data pulses at 1550 nm. The CW probe at 1542 nm and the pump pulses were injected into the integrated turbo-switch. The input powers were –2 and 6 dBm for the pump and probe respectively. The applied currents to SOA1 and SOA2 were 270 and 350 mA respectively.

One DI was applied to inverse the polarity of the output signal, which was composed of a piece of polarization maintaining fiber (PMF) of 3 m, with a differential delay of 3 ps and a polarizer. Figure 12 shows the eye diagrams of input data and wavelength-converted output signal at 84.8 Gbit/s respectively. Due to the imperfect input data signal from the passive optical multiplexer, the eye diagram of the input was not exactly uniform in amplitude, however the eye diagram of the output did reproduced the original one, and did not degraded after wavelength conversion, the optical signal-to-noise ratio (OSNR) was > 12 dB. Higher data-rate operation for 160 Gbit/s is under way. The eye diagram indicates the good performance of the wavelength conversion based on the integrated turbo-switch. Above all, these initial demonstrations have verified the feasibility of the proposed integrated turbo-switch at the first stage.

6 Conclusions

Turbo-switch has the capability of increasing the switching speed by a factor of four if compared with the case of a single SOA. The overall recovery time and the bandwidth of turbo-switch were extensively analyzed to explore its ultimate operation speed. The frequency-domain analysis

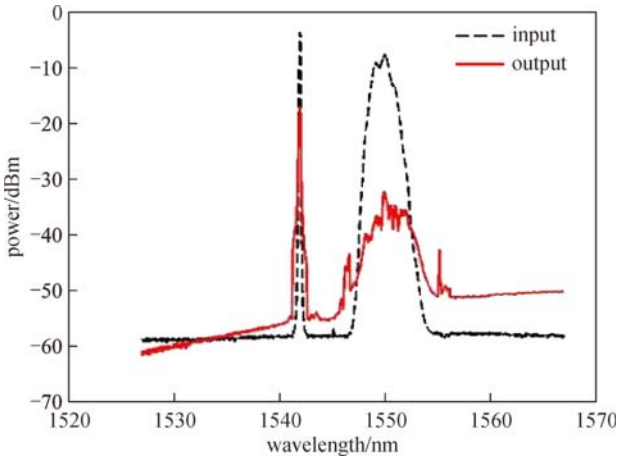

Fig. 8 Spectra of the pump (2 ps pulses, FWHM) and probe (CW) optical signals before and after MZI

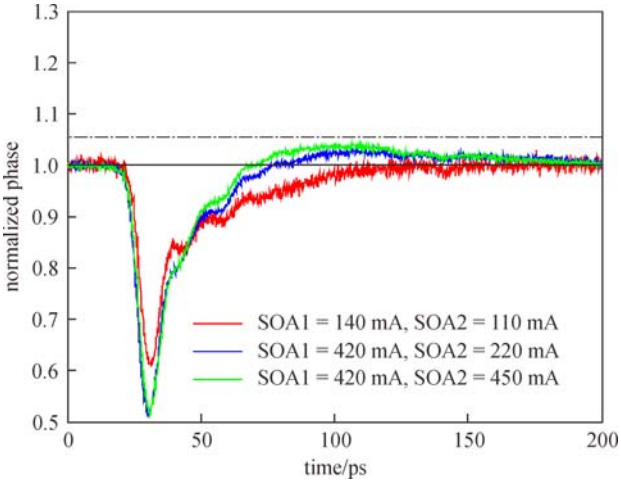

Fig. 9 Gain dynamics measurements of the integrated turbo-switch under different SOA bias currents

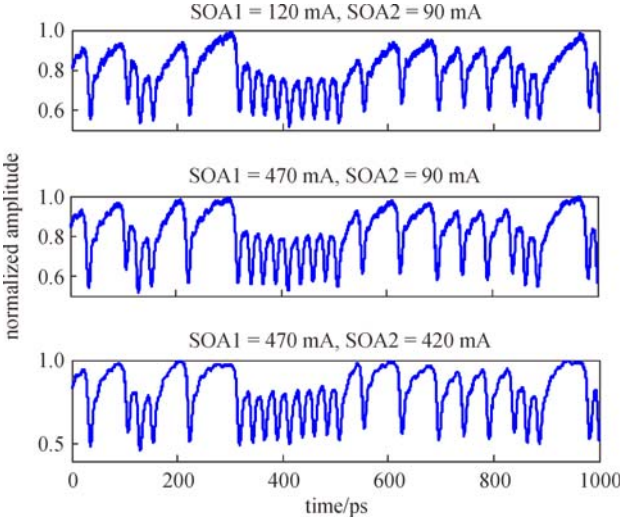

Fig. 10 Waveforms of CW modulated signal by 42.4 Gbit/s pump data pulses under different SOA bias currents

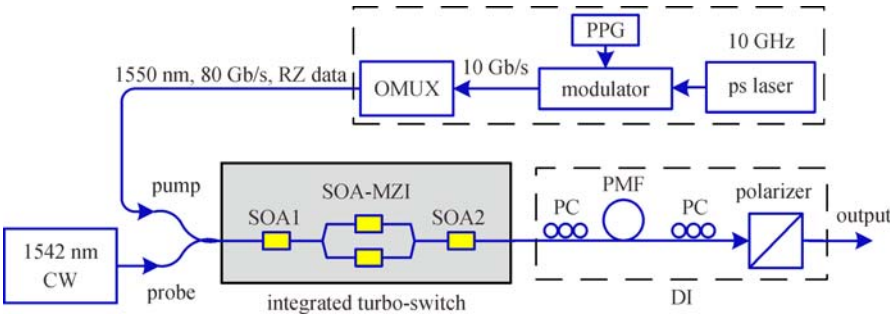

Fig. 11 Experimental setup of wavelength conversion using integrated turbo-switch

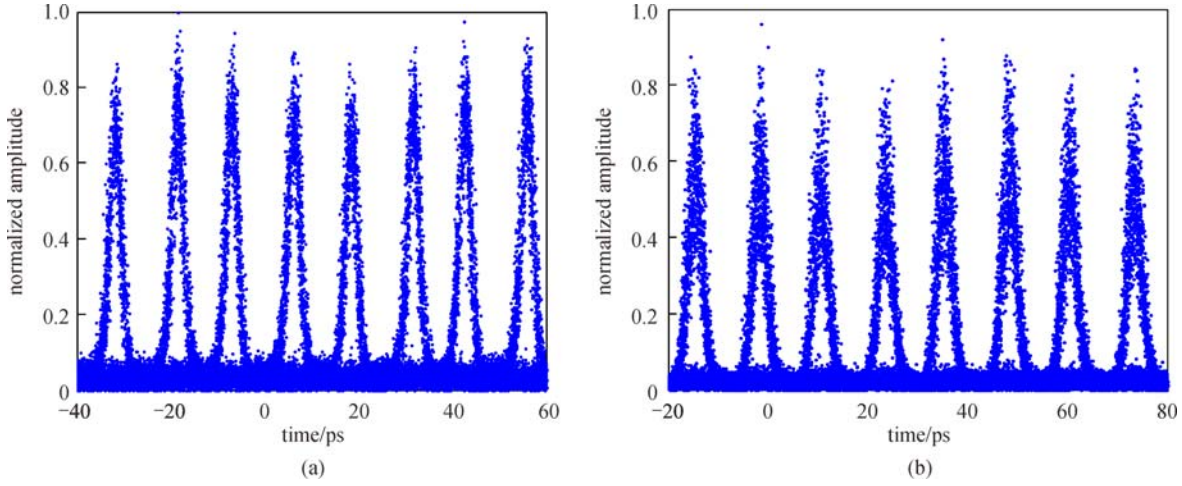

Fig. 12 Eye diagrams of wavelength conversion at 84.8 Gbit/s. (a) Input, and (b) output signals

suggests turbo-switch can be operated more than 300 Gbit/s. In addition, an integrated turbo-switch was first proposed and demonstrated, where a SOA-MZI was implemented as an optical band-pass filter. The gain dynamics and pattern effect were in good agreement with the reported experimental results of turbo-switch based on discrete SOAs. All-optical wavelength conversion based on the turbo-switch was demonstrated at 84.8 Gbit/s. Furthermore, the integrated turbo-switch becomes more stable and reliable in performance, which could be a good candidate for all-optical high-speed signal processing.

Acknowledgements This work was supported in part by the National Program on Key Basic Research Project (No. 2012CB315602), the National Natural Science Foundation of China (Grant Nos. 61571291, 61431009, 61221001 and 61132004) , and International S&T Cooperation Program of China (No. S2016G8017).

References

1. Yang X, Manning R J,Webb R P. All-optical 85Gb/s XOR using dual ultrafast nonlinear interferometers and turbo-switch configuration. In: Proceedings of Europe Conference on Optical Communication (ECOC), 2006, 1–2
2. Liu Y, Tangdiongga E, Li Z, de Waardt H, Koonen A M J, Khoe G D, Shu X, Bennion I, Dorren H J S.Error-free 320-Gb/s all-optical wavelength conversion using a single semiconductor optical amplifier. Journal of Lightwave Technology, 2007, 25(1): 103–108
3. Manning R J, Yang X, Webb R P, Giller R, Gunning F C G, Ellis A D. The turbo-switch – a novel technique to increase the high-speed response of SOAs for wavelength conversion. In: Proceedings of Optical Fiber Communication Conference (OFC), 2006, OSW8-1–OSW8-3
4. Weng Q, Yang X, Hu W.Theoretical analysis of high-speed all-optical turbo-switches. IEEE Journal of Selected Topics in Quantum Electronics, 2012, 18(2): 662–669
5. Mecozzi A, Mørk J. Saturation effects in non-degenerate four-wavemixing between short optical pulses in semiconductor laser amplifiers. IEEE Journal of Selected Topics in Quantum Electronics, 1997, 3(5): 1190–1207
6. Davies D A O. Small-signal analysis of wavelength conversion in semiconductor laser amplifiers via gain saturation. IEEE Photonics Technology Letters, 1995, 7(6): 617–619
7. Wang G, Wu C, Yang X, Hu W.Frequency-domain analysis of high-speed all-optical SOA-based turbo-switches. In: Proceedings of Asia Communications and Photonics Conference (ACP), 2012, AS2B.2-1–AS2B.2-3

8. Reid D A, Clarke A M, Yang X, Maher R, Webb R P, Manning R J, Barry L P.Characterization of a turbo-switch SOA wavelength converter using spectrographic pulse measurement. IEEE Journal of Selected Topics in Quantum Electronics, 2008, 14(3): 841–848
9. Manning R J, Yang X, Webb R P, Giller R, Cotter D. Cancellation of nonlinear patterning in semiconductor amplifier based switches. In: Proceedings of Optical Amplifiers & their Applications (OAA), 2006, OTuC1-1–OTuC1-3
10. Giller R, Yang X, Manning R J, Webb R P, Cotter D. Pattern effect mitigation in the turbo-switch. In: Proceedings of International Conference on Photonics in Switching, 2006, 1–3

Xuelin Yang received his Ph.D. degree from Shanghai Jiao Tong University in 1995. From Sept. 1999 to Sept. 2009, He was employed in Ecole Normale Superieure de Lyon in France, Eindhoven University of Technology in the Netherlands, Tyndall National Institute in Ireland and Bangor University in UK. Dr. Yang joined in Shanghai Jiao Tong University since 2009. His interests mainly focused on ultrafast all-optical signal processing in optical fiber communication, focused on applications of semiconductor optical amplifiers, security of optical networks, optical orthogonal frequency-division multiplexing (OFDM) transmission and passive optical networks (PONs).

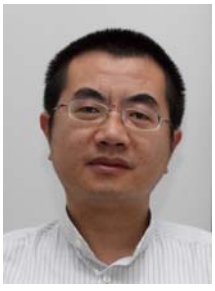

Weisheng Hu received his B.S, M.S, and Ph.D. degrees from Tsinghua University, Beijing, University of Science and Technology, and Nanjing University in 1986, 1989 and 1997 respectively. He is a full professor in Shanghai Jiao Tong University, and promoted to national second-level professor and distinguished professor in 2009. He served as the deputy director and director of State Key Laboratory of Advanced Optical Communication Systems and Networks between 2002 and 2012, and has been serving as the leader of Department of Electronic Engineering from 2013. Meanwhile, he serves on five journal editorial boards including *Optics Express*, *Journal of Lightwave Technology*, *Chinese Optics Letters*, *China Communications*, *Frontiers of Optoelectronics,* and a number of conference committees, including OFC, ICC, INFOCOM, OPTICSEAST.